Surface effects on the amplitude of fluctuation-induced interactions in smectic films

I. N. de Oliveira and M. L. Lyra
Departamento de Física, Universidade Federal de Alagoas, 57072-970 Maceió Alagoas, Brazil
(Received 20 December 2001; published 24 May 2002)

Within a quadratic functional integral approach, we investigate the role played by surface terms in the fluctuation-induced surface-surface interaction of free standing smectic liquid crystals. We show that the typical $1/l$ decay of the Casimir-type contribution to the free energy of a film with thickness l is replaced by a faster $1/l^3$ decay at a characteristic surface tension. An intermediate $1/l^2$ decay can also take place for specific surface parameters with unlike boundary conditions. In all the investigated cases, a repulsive long-range force appears only for mixed boundary conditions with strong anchoring at one surface and weak anchoring at the opposite one. Further, the amplitude of the thermal Casimir energy, besides being influenced by the applied surface tension, depicts a nonmonotonic dependence on the coupling between the outermost film layers, reflecting a crossover between strong and weak anchoring regimes.

DOI: 10.1103/PhysRevE.65.051711 PACS number(s): 61.30.Hn, 61.30.Dk, 64.70.Md

I. INTRODUCTION

Smectic liquid-crystal films are rich physical systems in which the interplay between surface and finite-size effects can be experimentally investigated. A stack of smectic layers confined by surrounding gas forms a free standing smectic film [1,2]. The effective coupling between the film and the gas is represented by a surface tension term, which reduces fluctuations in the smectic order and provides the characteristic quasi-long-range order with logarithmically diverging fluctuations. The reduced fluctuations near the film surface are related to several anomalous phenomena such as existence of smectic films at high temperatures as compared with bulk samples [3,4], surface-enhanced ordering, and layer-thinning transitions [5–7].

Fluctuations in liquid-crystal films with slowly decaying (power-law) correlations give rise to a fluctuation-induced long-range interaction between the film surfaces [8–14]. In the particular case of smectic-*A* films, this fluctuation-induced force decays as $1/l^2$, where l is the film thickness [8,9]. This thermal Pseudo-Casimir force has a longer range than the usual van der Waals interaction that decays as $1/l^3$ and is expected to play a relevant role governing phase transitions in free standing smectic films. This thermally induced interaction is attractive for like boundary conditions and repulsive otherwise. However, the amplitude of such interaction is not universal. For example, it was demonstrated that the interaction amplitude depends continuously on the applied surface tension even in the limit of very thick films [8]. This feature is in contrast to the general behavior at conventional critical points [15] as well as to that of long-range interactions induced by fluctuations of the orientational order in hexatic films [11]. In these systems, any finite anchoring is renormalized to the strong anchoring limit as the film thickness grows. The peculiar behavior of smectic-*A* films is due to the fact that it is the surface tension itself that stabilizes the quasi-long-range order and provokes the emergence of the Pseudo-Casimir force.

In the present work, we examine the fluctuation-induced interaction energy Δf between the surfaces of a layered smectic-*A* film within a quadratic functional-integral approach. By employing a subtraction scheme, we are able to obtain precise numerical values for the interaction energy of thin films within a discrete formulation. Also, in the limit of very thick films, our numerical results are in full agreement with those obtained within a continuum approach. The asymptotic amplitude of the interaction energy is computed as a function of the surface tension and the surface coupling constants. We will show that the nature of this long-range force is closely related to the profile of smectic fluctuations, which presents distinct trends for weak and strong anchoring.

II. SMECTIC-*A* FILMS: FLUCTUATIONS PROFILE AND THERMAL CASIMIR ENERGY

For a thin smectic-*A* film with N layers, the fluctuation Hamiltonian in the harmonic approximation is given by [1]

$$\mathcal{H}=\int_a^L d^2r\left[\sum_{i=1}^{N}\frac{dK_i}{2}[\triangle u_i(\mathbf{r})]^2+\sum_{i=1}^{N-1}\frac{B_i}{2d}[u_{i+1}(\mathbf{r})-u_i(\mathbf{r})]^2+\frac{\gamma_1}{2}|\nabla u_1(\mathbf{r})|^2+\frac{\gamma_N}{2}|\nabla u_N(\mathbf{r})|^2\right], \quad (1)$$

where $u_i(\mathbf{r})$ describes the displacement of the ith smectic layer from its original equilibrium position at point $\mathbf{r}$. Here d is the average distance between layers and a is a short-wavelength cutoff. γ_i is the surface tension between the external surfaces and the surrounding gas and accounts for the additional energy cost associated with increasing the surface area of the two free surfaces. Within the above Gaussian approximation, the surface tension acts by anchoring the surface layers of free standing films. It penalizes any gradient of the surface layer displacement, with the equilibrium direction being defined by the film holders used in the free standing technique [16]. B_i is the smectic elastic constant associated with the compression of layers $i+1$ and i, while K_i is the elastic constant associated with the bending of the ith layer. Close to the transition temperature, at which the smectic order is established, the elastic constants present a considerable dependence on the layer index i. Well inside the smectic phase, the elastic constants assume a more flat pro-

file and the only substantially distinct constants are those related to the surface ones [17]. Hereafter, we will restrict our analysis to this latter case assuming that the surface terms are K_S^1, K_S^N, $B_S^1=B_S^N=B_S$, while we keep all other elastic constants equal to the bulk values K and B. This model was first introduced by Holyst to compute the x-ray-diffraction pattern for thin smectic-A liquid-crystal films [18] and further extended by Mirantsev to allow for nonflat profiles of the elastic constants [17].

By employing a continuous Fourier transform with respect to **r**, the quadratic Hamiltonian is partially diagonalized resulting in the more compact form

$$\mathcal{H}=\frac{1}{2}\int_{2\pi/L}^{2\pi/a}\frac{d^2q}{(2\pi)^2}\left[\sum_{i,j=1}^{N}u_i(\mathbf{q})M_{i,j}u_j(-\mathbf{q})\right], \tag{2}$$

where the only nonzero elements of the matrix **M** are

$$M_{1,1}=\gamma_1 q^2+dK_S^1q^4+B_S/d, \tag{3}$$

$$M_{N,N}=\gamma_N q^2+dK_S^Nq^4+B_S/d, \tag{4}$$

$$M_{2,2}=M_{N-1,N-1}=dKq^4+(B_S+B)/d, \tag{5}$$

$$M_{i,i}=dKq^4+2B/d, \quad i\neq 1,2,N-1,N, \tag{6}$$

$$M_{1,2}=M_{2,1}=M_{N-1,N}=M_{N,N-1}=-B_S/d, \tag{7}$$

$$M_{i,i+1}=M_{i+1,i}=-B/d, \quad i\neq 1,N-1. \tag{8}$$

The quadratic form of the Hamiltonian yields simple expressions for some thermodynamic quantities of interest. In particular, we will compute the average layer displacement fluctuations

$$\sigma_i^2=\langle u_i^2\rangle=k_BT\int\frac{d^2q}{(2\pi)^2}(M^{-1})_{i,i}, \tag{9}$$

and the total free energy

$$\frac{f}{k_BT}=\frac{1}{2}\int\frac{d^2q}{(2\pi)^2}\sum_m\ln\lambda_m=\frac{1}{2}\int\frac{d^2q}{(2\pi)^2}\ln\det\mathbf{M}, \tag{10}$$

for which standard matrix algebra can be used to compute $(M^{-1})_{i,i}$, $\det\mathbf{M}$ and the eigenvalues λ_m [11,18,19].

Some aspects related to the displacement fluctuations profile have already been reported in the literature for the regime of strong anchoring, i.e., surface tensions larger than a characteristic tension $\gamma_c=\sqrt{KB}$ [18]. Here, we stress some features related to the weak anchoring regime and to the film thickness and surface tension dependence of the average displacement fluctuation $\sigma=\sqrt{\langle\sigma_i^2\rangle}$. These will be shown to play an important role in the physical interpretation of the behavior of the fluctuation-induced long-range interaction between the film surfaces.

In Fig. 1, we show our results for the profile of smectic fluctuations on a 41-layer film as obtained from direct integration of Eq. (9) for films with $\gamma_1=\gamma_N=\gamma$ (only half of the symmetric profile is depicted). We used typical values for the elastic constants $K=1\times10^{-6}$ dyn and $B=2.5\times10^7$ dyn/cm^2. Further, we considered $d=30$ Å, $a=4$ Å, $L=1$ cm, $k_BT=4\times10^{-14}$ erg. The most relevant surface ordering term is the one related to the surface-gas tension. For strong anchoring the fluctuation profile has a negative concavity. In this regime, the surface tension strongly reduces surface fluctuations thus overcoming the effect of the presence of open boundaries. For weak anchoring, however, the fluctuation profile changes to a positive concavity. In this case, although the surface tension still acts inducing quasi-long-range order, the open boundaries effect dominates, making the inner layers more robust than the outer ones. The layer fluctuations assume an almost flat profile at the characteristic surface tension γ_c with a small downward curvature near the surfaces when $K_S=K$. By tuning the surface Frank constants to $K_S=K/2$, a flatter profile near the surfaces can be obtained, with the surface layers exhibiting a slightly larger displacement fluctuation than the inner ones.

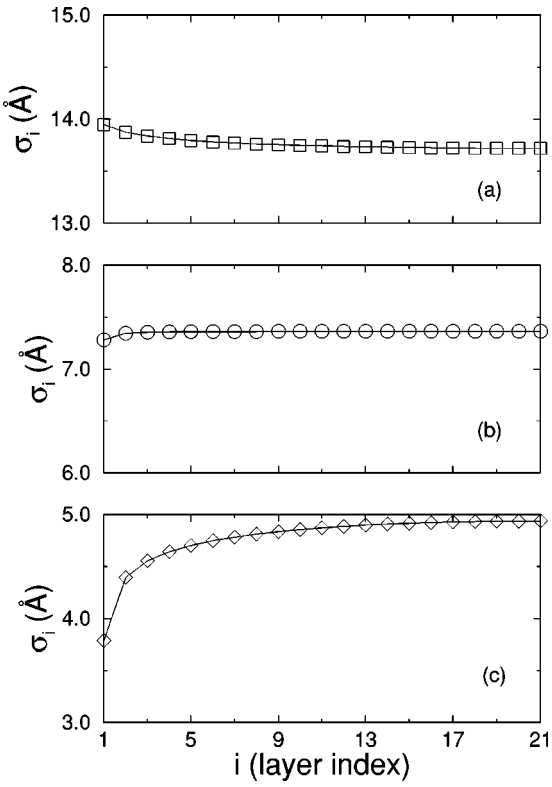

FIG. 1. Profile of smectic fluctuations for a 41-layer film. The bulk and surface constants were kept equal to the experimentally typical values $K=1\times10^{-6}$ dyn and $B=2.5\times10^7$ dyn/cm^2, for which the characteristic surface tension is $\gamma_c=\sqrt{KB}=5$ dyn/cm. The surface tensions are (a) $\gamma=5\gamma_c$; (b) $\gamma=\gamma_c$; and (c) $\gamma=\gamma_c/5$. Notice that the smectic fluctuations change from a positive curvature profile for $\gamma<\gamma_c$ to a negative curvature profile for $\gamma>\gamma_c$. These data were obtained for like boundary conditions ($\gamma=\gamma_1=\gamma_N$).

The above results show that the smectic fluctuation profile has an overall negative curvature when both surface tensions are greater than γ_c (strong anchoring regime). With both surface tensions smaller than γ_c (weak anchoring regime), an overall positive curvature takes place characterizing the

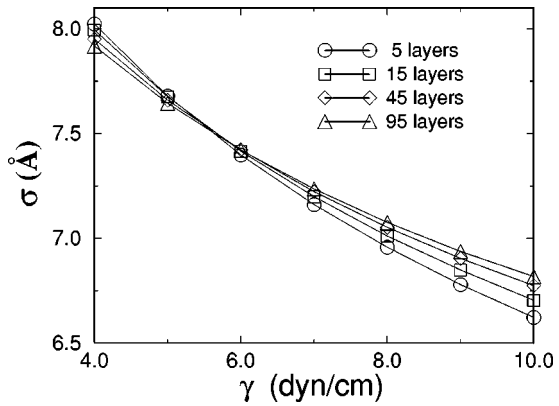

FIG. 2. Average fluctuation σ of a smectic film vs the surface tension γ for several film thicknesses. Coupling constants are the same as in Fig. 1. For strong anchoring ($\gamma > \gamma_c$) the average fluctuation grows with the film thickness once bulk layers fluctuate more than the strongly constrained surface ones. For weak anchoring ($\gamma < \gamma_c$) this trend is reversed because the presence of open boundaries undertakes the anchoring and surface layers are those exhibiting larger fluctuations.

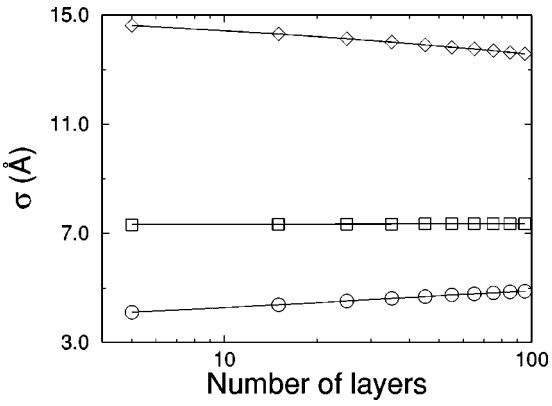

FIG. 3. Average fluctuation σ vs film thickness for typical surface tensions. Coupling constants are the same as in Fig. 1. For $\gamma = \gamma_c$ (squares) the average fluctuation is roughly thickness independent. For $\gamma = 5\gamma_c$ (circles) the average fluctuation grows with film thickness reflecting the dominant role played by surface anchoring. For $\gamma = \gamma_c/5$ (diamonds) the average fluctuation decreases with film thickness as the presence of open boundaries has a predominant role in the weak anchoring regime.

weak anchoring regime. For mixed boundary conditions with strong anchoring in one surface and weak anchoring in the opposite one, the profile presents an inflexion point near the center, i.e., an upward curvature in the film side under weak anchoring and a downward curvature at the side under strong anchoring. We call attention to these features since they will be shown to be strongly correlated with the attractive or repulsive nature of the fluctuation-induced interaction between the film surfaces.

The reported change in the concavity of the fluctuation profile is characteristic of surface ordering fields that induce quasi-long-range order. In contrast, surface terms that do not induce a new order, such as enhanced surface elastic constants in hexatic films, are only effective at distances smaller than a characteristic length and do not change the profile curvature at the bulk of thick films. On the other hand, surface ordering fields that induce true long-range order have a dominant effect at the bulk fluctuations even in the limit of weak anchoring [19].

This change in the fluctuation profile is reflected in the average fluctuation of the smectic order σ. In Fig. 2, we plot σ as a function of the surface tension for several film thicknesses. At weak anchoring $\gamma < \gamma_c$ thicker films have smaller fluctuations as bulk layers are more ordered. On the other hand, in the regime of strong anchoring $\gamma > \gamma_c$, thin films exhibit a more robust smectic order. Similar data are presented in Fig. 3 where these distinct trends are more clearly depicted.

The total free energy of a film with open boundaries and thickness l has the following functional dependence on l:

$$f = l f_B + f_S + \Delta f(l), \tag{11}$$

where $l f_B$ is the extensive part, proportional to the number of layers. In the limit of $l \to \infty$, f_B gives the bulk free energy density. f_S is the surface contribution and $\Delta f(l)$ is the fluctuation-induced interaction energy that vanishes as $l \to \infty$.

In the limit where the number of smectic layers $N \to \infty$ but with $l = (N-1)d$ finite, a simple expression for the interaction energy can be obtained from the continuous version of the model [8]. Here we draw the main lines of such derivation with an extension to the case of films with enhanced surface Frank constants K_S^1 and K_S^N. The surface elastic constant will be kept equal to the bulk one allowing us to find a closed expression for Δf. The general case of $B_S \neq B$ will be discussed later. It is straightforward to show that, in the continuous regime, the eigenmodes are obtained from the differential equation,

$$dKq^4 u(z) - dB \frac{\partial^2 u(z)}{\partial z^2} = \lambda u(z), \tag{12}$$

where z runs from 0 to l. The eigenmodes have to satisfy the boundary conditions,

$$(dK_S^1 q^4 + \gamma_1 q^2) u(0) - B \left(\frac{\partial u}{\partial z} \right)_{z = d/2} = \lambda u(0), \tag{13}$$

$$(dK_S^N q^4 + \gamma_N q^2) u(l) + B \left(\frac{\partial u}{\partial z} \right)_{z = l - d/2} = \lambda u(l). \tag{14}$$

Although $d \ll l$ in the continuous limit, we need to keep it explicitly in the boundary conditions to obtain the correct asymptotic dependence of Δf on the elastic Frank constants K and K_S^i. The eigenvalues λ_m subject to the above boundary conditions have the form

$$\lambda_m = dKq^4 + \frac{B}{d} \omega(m)^2, \tag{15}$$

where $\omega(m)$ are the solutions of

$$\omega(m)(l/d)+\arctan\phi_1+\arctan\phi_N=m\pi \quad (m=0,1,\ldots), \tag{16}$$

with

$$\phi_i=\frac{(B/d)\omega(m)^2-\gamma_i q^2-d(K_S^i-K)q^4}{(B/d)\omega(m)}-\frac{\omega(m)}{2}, \tag{17}$$

where terms of higher order in $\omega(m)$ were neglected. The volume and surface terms of the free energy in Eq. (10) are formally divergent in the continuous limit. We can compute the interaction energy by applying the Poisson summation formula [20], which naturally splits the surface and volume terms and replaces the discrete summation over m by an integral over ω [8,19]. After some algebra, we obtain

$$\Delta f(l)=\frac{k_BT}{2}\int\frac{d^2q}{(2\pi)^2}\ln[1-e^{-2l\sqrt{K/B}q^2}G_1G_N], \tag{18}$$

where

$$G_i=\frac{(\gamma_c-\gamma_i)q^2-d(K_S^i-K/2)q^4}{(\gamma_c+\gamma_i)q^2+d(K_S^i-K/2)q^4}, \tag{19}$$

γ_1 and γ_N being the surface tensions on each film surface. Keeping the dominant term of Eq. (18) for large l, the interaction energy can be shown to decay asymptotically as $1/l$ on the form

$$\lambda_c d\frac{\Delta f(l)}{k_BT}=\Delta\left(\frac{d}{l}\right), \tag{20}$$

where the characteristic smectic length $\lambda_c=\sqrt{K/B}$ and the surface tension dependent amplitude Δ is given by

$$\Delta=-\frac{1}{16\pi}\sum_{n=1}^{\infty}\left[\left(\frac{\gamma_c-\gamma_1}{\gamma_c+\gamma_1}\right)\left(\frac{\gamma_c-\gamma_N}{\gamma_c+\gamma_N}\right)\right]^n\frac{1}{n^2}. \tag{21}$$

Notice that the asymptotic amplitude is independent of the surface Frank constants K_S^i.

In the discrete model, the interaction energy has to be obtained from direct integration of Eq. (10) after computing $\det\mathbf{M}$ through algebraic methods. Further, a subtraction scheme has to be numerically implemented to separate the fluctuation-induced contribution for the free energy. The matrix algebra is quite similar to that used to investigate the free energy of hexatic films [see Eqs. (5)–(7) of Ref. [19]]. The extensive contribution coming from the analytical expression for $\ln\det\mathbf{M}$ can be quite easily identified and isolated so that we effectively just need to numerically compute $f_s+\Delta f(l)$. In order to obtain the surface term, we compute the free energy in the limit of $l\to\infty$ for which the fluctuation term is absent. The above procedure allows us to compute the fluctuation-induced interaction even in the limit of very thin films and to identify corrections to scaling to the asymptotic expression. Also, we can account for the relative effect of having distinct surface couplings.

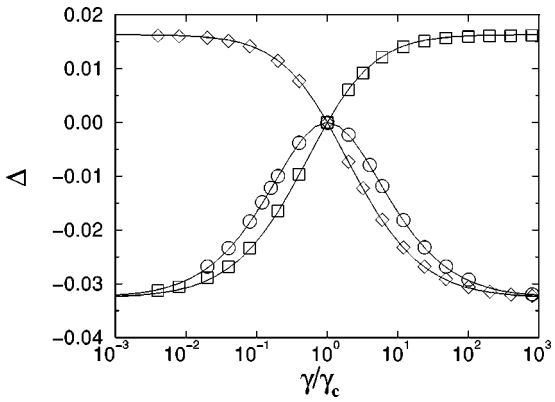

FIG. 4. The asymptotic amplitude Δ of the fluctuation-induced interaction energy vs the surface tension as obtained from the numerical integration of Eq. (10) followed by a subtraction scheme. Coupling constants are the same as in Fig. 1. Circles are data for like boundary conditions $\gamma_1=\gamma_N=\gamma$. Two unlike boundary conditions were considered: $\gamma_1=0$ and $\gamma_N=\gamma$ (squares); $\gamma_1\to\infty$ and $\gamma_N=\gamma$ (diamonds). The solid lines are the resulting expressions for Δ obtained by the continuous version of the model. Notice that the long-range fluctuation-induced force is attractive whenever one has strong anchoring ($\gamma>\gamma_c$) or weak anchoring ($\gamma<\gamma_c$) at both surfaces. For mixed anchoring a repulsive interaction takes place.

In Fig. 4, we present our numerical results for the amplitude of the fluctuation-induced interaction in the limit of very thick films and compare it with the expression obtained from the continuous model. Both results coincide within the accuracy of the numerical procedure. The corresponding fluctuation-induced force is attractive whenever strong anchoring ($\gamma>\gamma_c$) or weak anchoring ($\gamma<\gamma_c$) is imposed on both film surfaces. On the other hand, a repulsive interaction takes place for mixed anchoring. This behavior can be correlated to the profile of smectic fluctuations that for mixed anchoring exhibits an inflexion point. Therefore, for smectic-*A* films, fluctuation profiles with a positive or negative curvature generate an attractive long-range interaction between the film surfaces, whereas profiles exhibiting an inflexion point (mixed boundary conditions) result in a repulsive long-range force. The amplitude vanishes whenever one of the surface tensions are equal to the characteristic tension γ_c. This feature reflects a faster decay of the fluctuation-induced interaction in these cases.

In Fig. 5, we plot the interaction energy vs the film thickness (in units of layer spacing) for the case of like boundaries and several surface tensions. Indeed, we find that at $\gamma=\gamma_c$ a faster decay of the fluctuation-induced interaction takes place with $\Delta f(l)\propto 1/l^3$. Expanding Eq. (18) after imposing $\gamma_1=\gamma_N=\gamma_c$ but allowing distinct surface Frank constants, we find that

$$\lambda_c d\frac{\Delta f(l)}{k_BT}=-\frac{1}{128\pi}\left(\frac{K_S^1-K/2}{K}\right)\left(\frac{K_S^N-K/2}{K}\right)\left(\frac{d}{l}\right)^3, \tag{22}$$

which now explicitly depends on the surface Frank constants. The equation above is in full agreement with the numerical results. The interaction amplitude vanishes when ei-

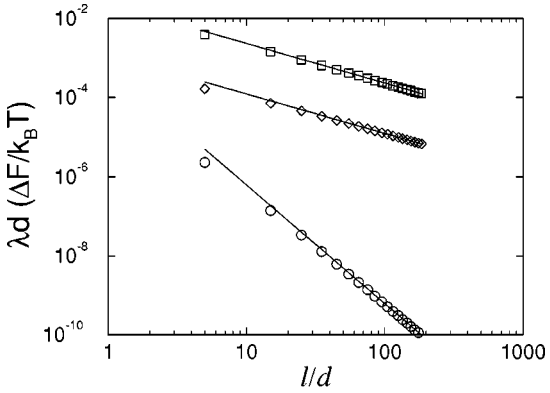

FIG. 5. The fluctuation-induced interaction energy vs film thickness (in units of the average layer spacement d) for several surface tensions and like boundary conditions with $K_S=K$. Notice that the asymptotic scaling regime of $\Delta f \propto 1/l$ takes place at general surface tensions [$\gamma=120$ dyn/cm(squares) and $\gamma=3$ dyn/cm(diamonds)] with small corrections to scaling for thin films. At the characteristic surface tension (circles) a faster decay takes place with $\Delta f \propto 1/l^3$. The amplitude in this case is in full agreement with the continuous limit result [Eq. (22)].

ther K_S^1 or K_S^N (or both) equals to $K/2$. In these cases, we observed numerically that Δf displays a faster $1/l^4$ decay (when only one of the surface Frank constants equals $K/2$) and an even faster $1/l^5$ decay for $K_S^1=K_S^N=K/2$. This particular value of $K_S=K/2$ and $\gamma=\gamma_c$ corresponds to the parameter set for which the fluctuations profile is quite flat even very close to the film surfaces. The small downward curvature depicted in Fig. 1(b) changes to an upward one for $K_S<K/2$. Also in this limiting case, repulsive interaction force occurs only for mixed boundary conditions, i.e., a strong Frank constant at one surface and a weak Frank constant at the opposite one.

The fluctuation-induced interaction for the case of unlike boundaries with $\gamma_1=\gamma_c$ as a function of γ_N takes the asymptotic form

$$\lambda_c d \frac{\Delta f(l)}{k_B T} = \Delta' \left(\frac{d}{l}\right)^2, \tag{23}$$

where

$$\Delta' = -\frac{1}{64\pi}\left(\frac{K_S-K/2}{K}\right)\left(\frac{\gamma_N-\gamma_c}{\gamma_N+\gamma_c}\right) \tag{24}$$

and, therefore, exhibits an intermediate $1/l^2$ decay. Notice that its nature is also attractive for strong ($K_S>K/2, \gamma_N>\gamma_c$) and weak ($K_S<K/2, \gamma_N<\gamma_c$) anchoring at both surfaces, becoming repulsive for mixed boundary conditions. The interaction amplitude for this latter case is illustrated in Fig. 6 together with numerical data.

The effect of distinct elastic coupling constants B_S acting in the film surfaces can be explored numerically. Contrary to the surface Frank constant that do not influence the asymptotic amplitude of the fluctuation-induced interaction in the general case of $\gamma \neq \gamma_c$, we found B_S to strongly modify the interaction amplitude. The surface elastic constant effectively governs how the surface ordering induced by the surface tension can be propagated to the inner layers. If B_S is small, only a partial ordering is transmitted and the film behaves such as in the weak anchoring regime. For large B_S, the surface ordering is efficiently transmitted. In Fig. 7 we show the behavior of the asymptotic amplitude of the fluctuation-induced interaction energy as a function of the surface elastic constant for distinct values of the surface tension and in the case of like boundaries. In the regime of weak anchoring ($\gamma<\gamma_c$) the absolute value of the amplitude Δ increases with decreasing B_S once the system becomes effectively less anchored. In the opposite case of strong anchoring ($\gamma>\gamma_c$) the absolute value of Δ reaches a minimum with increasing B_S, which, according to the results shown in Fig. 4, characterizes the crossover from weak to strong anchoring. However, the interaction amplitude Δ does not vanish except at the particular case of $\gamma=\gamma_c$.

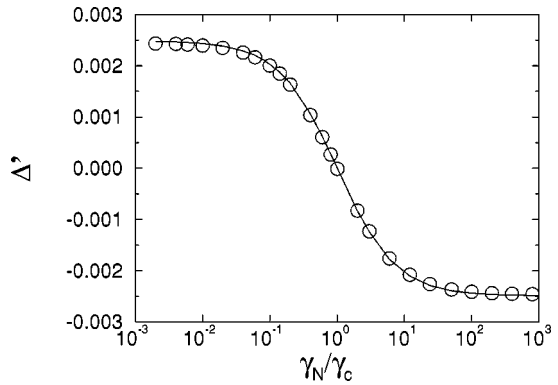

FIG. 6. The asymptotic amplitude Δ' of the fluctuation induced interaction versus surface tension for $\gamma_1=\gamma_c$ and $\gamma_N=\gamma$. Here we used $K_S=K$. The numerical data agree with the expression [Eq. (24)] obtained from the continuous model (solid line).

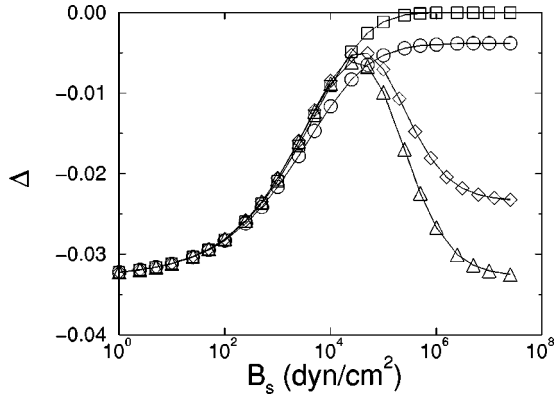

FIG. 7. The asymptotic amplitude Δ of the fluctuation-induced interaction energy vs the surface coupling B_S for like boundary conditions and typical surface tensions. For weak anchoring $\gamma=2$ dyn/cm(circles) the amplitude Δ continuously decreases with decreasing B_S once the film effectively becomes even weakly anchored. A similar trend extends up to $\gamma=\gamma_c$(squares). For strong anchoring [$\gamma=60\,000$ dyn/cm(triangles) and $\gamma=120$ dyn/cm(diamonds)] the amplitude Δ exhibits a nonmonotonic behavior reflecting the crossover from strong anchoring to weak anchoring as the surface coupling is decreased.

III. SUMMARY AND CONCLUSIONS

In this work, we used a quadratic functional approach for the Hamiltonian of free standing smectic films of thickness l to compute the fluctuation-induced interaction between the film surfaces for several regimes of anchoring. By using matrix algebra together with direct numerical integration, we reproduced the well known $1/l$ dependence of the interaction energy as obtained by a continuous version of the model. The attractive nature of the interaction holds when strong or weak anchoring regimes are imposed on both film surfaces. For mixed boundary conditions (strong anchoring at one surface and weak anchoring at the opposite one), a repulsive fluctuation-induced interaction occurs. According to wetting theory, a repulsive interaction leads to a scenario where complete wetting is possible, whereas layer-by-layer wetting can take place for attractive interactions. The fluctuation profile depicts a vanishing curvature at the bulk when the surface tension is tuned to the characteristic value $\gamma_c=\sqrt{KB}$ that delimits the strong and weak anchoring regimes. We showed that, in this case, the fluctuation-induced interaction exhibits a faster decay becoming proportional to $1/l^2$ when the surface tension is tuned at only one film surface. A faster $1/l^3$ decay survives when the surface tension is tuned at γ_c on both surfaces. We reported analytical expressions for the asymptotic amplitude of the interaction energy on all relevant cases. Further, we showed that the interaction amplitude strongly depends on the elastic coupling between the film surfaces and the inner layers and that, in the case of large surface tensions and like boundary conditions, its absolute value exhibits a minimum characterizing the crossover from weak to strong anchoring.

ACKNOWLEDGMENTS

We would like to thank G.M. Viswanathan, R.J.V. dos Santos, and H.R. da Cruz for fruitful discussions and for the critical reading of the manuscript. This work was partially supported by the Brazilian research agencies CNPq (Conselho Nacional de Pesquisa) and CAPES (Coordenação de Aperfeiçoamento de Pessoal do Ensino Superior), and by the Alagoas State agency FAPEAL (Fundação de Amparo a Pesquisa do Estado de Alagoas). I.N.O. acknowledges financial support from CNPq.

[1] P.G. De Gennes and J. Prost, *The Physics of Liquid Crystals* (Clarendon Press, Oxford, 1993).
[2] S. Chandrasekhar, *Liquid Crystals* (Cambridge University Press, Cambridge, 1977).
[3] C. Rosenblatt and N.M. Amer, Appl. Phys. Lett. **36**, 432 (1980).
[4] S. Heinekamp, R.A. Pelcovits, E. Fontes, E.Y. Chen, R. Pindak, and R.B. Meyer, Phys. Rev. Lett. **52**, 1017 (1984).
[5] C. Bahr, Int. J. Mod. Phys. B **8**, 3051 (1994).
[6] T. Stoebe, P. Mach, and C.C. Huang, Phys. Rev. Lett. **73**, 1384 (1994).
[7] Y. Martínez–Ratón, A.M. Somoza, L. Mederos, and D.E. Sullivan, Phys. Rev. E **55**, 2030 (1997).
[8] L.V. Mikheev, Zh. Éksp. Teor. Fiz. **96**, 632 (1989) [Sov. Phys. JETP **69**, 358 (1989)].
[9] A. Ajdari, L. Peliti, and J. Prost, Phys. Rev. Lett. **66**, 1481 (1991).
[10] H. Li and M. Kardar, Phys. Rev. Lett. **67**, 3275 (1991).
[11] M.L. Lyra, M. Kardar, and N.F. Svaiter, Phys. Rev. E **47**, 3456 (1993).
[12] B.D. Swanson and L.B. Sorensen, Phys. Rev. Lett. **75**, 3293 (1995).
[13] P. Ziherl, R. Podgornik, and S. Zumer, Phys. Rev. Lett. **84**, 1228 (2000).
[14] P. Ziherl, F. Karimi Pour Haddadan, R. Podgornik, and S. Zumer, Phys. Rev. E **61**, 5361 (2000).
[15] M. Krech, J. Phys.: Condens. Matter **11**, R391 (1999).
[16] J. Collett, L.B. Sorensen, P.S. Pershan, and J. Als-Nielsen, Phys. Rev. A **32**, 1036 (1985).
[17] L.V. Mirantsev, Phys. Rev. E **62**, 647 (2000).
[18] R. Holyst, D.J. Tweet, and L.B. Sorensen, Phys. Rev. Lett. **65**, 2153 (1990); R. Holyst, Phys. Rev. A **44**, 3692 (1991).
[19] M.L. Lyra, Phys. Rev. B **47**, 2501 (1993).
[20] G. A. Korn and T. M. Korn, *Mathematical Handbook for Scientists and Engineers* (McGraw-Hill, New York, 1968).